Electronic Materials Letters, Vol. 2, No. 1 (2006), pp. 43-48

Effects of Nitrogen Addition on the Properties of Ge-Doped SbTe Phase Change Memory Material

Byung-ki Cheong[1]*, In Ho Kim[1], Hanju Jung[1,2], Taek Sung Lee[1], Jeung-hyun Jeong[1], Dae-Hwan Kang[1], Won Mok Kim[1], and Jae-Geun Ha[2]

[1]Thin Film Materials Research Center, Korea Institute of Science and Technology,
39-1 Hawolgok-dong, Sungbuk-gu, Seoul 136-791, Korea
[2]Department of Electronic Materials Engineering, Kwangwoon University,
447-1 Wolgye-1-dong, Nowon-gu, Seoul 139-701, Korea

Reduction of reset current and suppression of thermal interference between memory cells are considered to pose major technical challenges to the development of successful high-density phase-change memory devices. To overcome these challenges, a memory device may need a phase-change material featuring a low melting temperature combined with a high crystallization temperature. In this report, we propose a candidate material system, consisting of Ge-doped SbTe for a base material and nitrogen for a complementary property-modifier. Nitrogen-added Ge-doped SbTe materials were characterized to show that, with an increase in nitrogen content; melting temperature remains nearly constant and lower than that of $Ge_2Sb_2Te_5$; the crystallization temperature increases; and the electrical resistivities increase for as-deposited and annealed materials as well. In addition, the proposed materials were found to have excellent scaling characteristics in terms of crystallization speed. The observed property changes are discussed in relation to growth-dominant crystallization and the varying mode of nitrogen accommodation between intra- and inter-granular modes, and through comparison with a case of N-doped $Ge_2Sb_2Te_5$ material.

Keywords: non-volatile memory, phase-change memory material, Ge-doped SbTe, nitrogen addition, melting, crystallization

1. INTRODUCTION

Phase-change random access memory (PCRAM) is under active development toward commercialization and promises to be a leading high-performance nonvolatile memory. To date, PCRAM prototypes have made use of $Ge_2Sb_2Te_5$-based materials as memory materials[1-3]. It is uncertain, however, whether these same materials may be appropriate for a higher density PCRAM, which would have a cell size much smaller than that of today's device. Behind this uncertainty, there stand two major technical issues to deal with for the development of a higher density device. The first issue involves the reduction of reset current. The latest 64Mb PCRAM prototype[3] already uses a modified $Ge_2Sb_2Te_5$ material doped with nitrogen to reduce the reset current by way of enhanced Joule heating owing to the increased resistivity of the memory material. Conceivably, a higher-density PCRAM device may need a new memory material that has more suitable material properties than $Ge_2Sb_2Te_5$ for ever-decreasing reset current. The second issue involves the suppression of thermal interference between neighboring memory cells and, accordingly, of degrading data retention that would get worse with density growth particularly beyond the technology node of 45 nm[4]. To be able to deal effectively with the aforementioned issues, therefore, we may have to employ a memory material with such primary attributes as a lower melting temperature and a higher crystallization temperature as compared with the present $Ge_2Sb_2Te_5$ material.

A phase-change material system that has a minimum congruent melting point or a eutectic melting point according to its equilibrium phase diagram may be a good candidate for a future memory material. An example of such materials are Ge-doped Sb-Te's, which have been utilized in Blu-ray Discs as phase-change optical recording materials and very recently in a novel PCRAM device named phase-change line memory by Phillips[5]. From previous reports, these materials are found to have a melting temperature of around 550 °C and a crystallization temperature of around 170 °C, evidently in line with the requirements set out above[5,6]. Nevertheless,

*Corresponding author: bkcheong@kist.re.kr

crystalline Ge-doped Sb-Te materials tend to have lower electrical resistivities than $Ge_2Sb_2Te_5$ presumably due to a higher content of a metallic component, Sb, which would have an adverse effect on the reduction of reset current. A solution may be provided by the addition of an element that would lead to an increase in electrical and/or thermal resistivity. In the present study, we have chosen nitrogen for this purpose. As it turns out, the inclusion of nitrogen increases not only the electrical resistivity of a Ge-doped SbTe material but also the crystallization temperature, while tending to maintain the melting temperature. Herein, we report the results of our preliminary study of the material properties of Ge-doped SbTe with a nitrogen addition in terms of its potential for use in a higher density PCRAM.

2. EXPERIMENT

Thin films of a Ge-doped SbTe of varying nitrogen content were deposited via reactive RF magnetron sputtering using a target with a composition of $Ge_5Sb_{75}Te_{20}$ (in at.%) and sputter gases that consisted of ($Ar+N_2$) mixtures of varying N_2 content, from 0 to 12% (expressed in terms of percentile ratio of N_2 gas flow rate with respect to the total sputter gas flow rate). Sputtering was conducted at 2 mTorr and at a fixed power of 25W to yield a deposition rate of 0.17 nm/s. A cursory analysis of the nitrogen contents of the thin films was carried out with Rutherford backscattering spectrometry at nitrogen resonance (3.701 MeV He^{++}) and by use of the composition of a Ge-doped SbTe thick film predetermined from an inductively coupled plasma analysis. A fairly linear relationship was confirmed to exist between the nitrogen content of a film (in at%) and the N_2 gas flow ratio up to around 12%. For thermal analysis of the sputtered films by differential scanning calorimetry (DSC), films of 2 μm thickness were deposited on flexible stainless foils, which were then crumpled to collect film debris. The DSC runs were made with a NETZSCH DSC 204 at a fixed scanning rate of 10 °C/min. For Hall measurement and for structural characterization by x-ray diffractometry, films of 50 nm thickness on Corning glass substrates were utilized either in as-deposited amorphous states or after rapid thermal annealing at 300 °C for 5 min in a furnace under an Ar atmosphere of 1 Torr. These measurements were carried out with a laboratory-made Hall measurement apparatus and an x-ray diffractometer (Rigaku ATX-G) using CuK_α radiation. Thin films fabricated with different N_2 gas flow ratios were also compared in terms of crystallization speed by measuring the complete crystallization times of the melt-quenched amorphous marks of varying sizes using a static tester equipped with a 685 nm heating laser and a 633 nm probe laser. Each test sample was made up of a four-layer film stack consisting of Al alloy (100 nm)/$ZnS.SiO_2$ (20 nm)/phase change material (20 nm)/$ZnS.SiO_2$ (145 nm) on a polycarbonate substrate, which was laser-annealed to a fully crystalline state before use. The film stack was designed to yield a proper optical contrast between the amorphous and crystalline state and rapid cooling characteristics to facilitate the formation of melt-quenched amorphous marks.

3. RESULTS AND DISCUSSIONS

3.1. Phase Change Temperatures

Figure 1 shows the DSC results for the films sputtered with different N_2 flow ratios; these results were obtained with a scanning rate of 10°C/min, respectively, using alumina pans (Fig. 1(b)) and more sensitive aluminum pans during complementary runs for temperatures ranging from room temperature to 450 °C (Fig. 1(a)). For each N_2 flow ratio, there appears an exothermic peak below 300 °C as well as an endothermic peak around 550 °C. Based on the phase diagram of the Sb-Te binary system[6] and x-ray diffraction data of the annealed films, shown below, these peaks are considered to result from crystallization and melting, respectively. Characteristically, the crystallization temperature increases in proportion to the N_2 flow ratio, but the melting temperature appears nearly unaltered.

A remarkable feature can be seen in Fig. 1(a): the crystallization peak not only shifts to a higher temperature side but also tends to get weaker with N_2 flow ratio, while another exothermic peak grows at an even higher temperature. The first peak almost vanishes eventually at 12% N_2 with a full growth of the broad second peak. From the tendency of these changes, it follows that the reactions responsible for the two exothermic peaks may be closely linked to each other, rather than separate. Furthermore, it is presumed that crystallization at a lower temperature may become gradually hindered with increasing N_2 flow ratio until higher temperature crystallization takes over. Some evidence for this can be obtained from

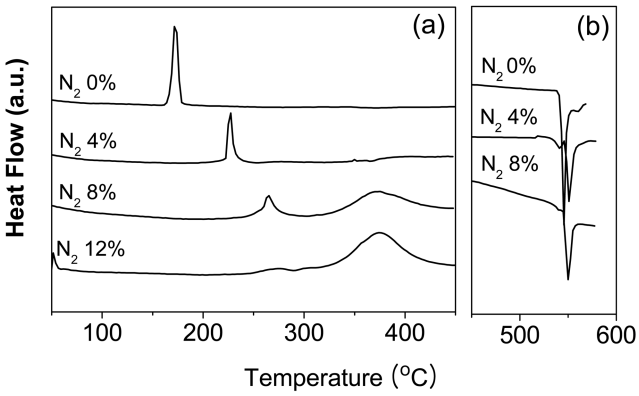

Fig. 1. DSC results obtained at the scanning rate of 10 °C/min for the films sputtered with varying N_2 gas flow ratios: (a) with aluminum pans, and (b) with alumina pans. Notice that crystallization temperature increases with N_2 flow ratio, but melting temperature appears nearly unaltered.

the results of the structural characterization presented below.

3.2. Structural Characteristics

Figure 2 shows the x-ray diffraction spectra taken from annealed films (annealed at 300 °C for 5 min.) fabricated at varying N_2 flow ratios along with one fabricated with 8% N_2 that was heated to 450 °C and then cooled to room temperature in the DSC chamber. Nearly all the x-ray peaks in Fig. 2 may be indexed according to a hexagonal crystal structure[7], including those of the DSC sample. This hexagonal crystal structure may be envisioned intuitively as being derived from a rocksalt-like structure[7] by symmetry-breaking distortion along one of the <111> axes. In fact, peaks having indexes 104 and 110, for example, would have merged into a single peak if the crystalline film had assumed a rocksalt-like structure.

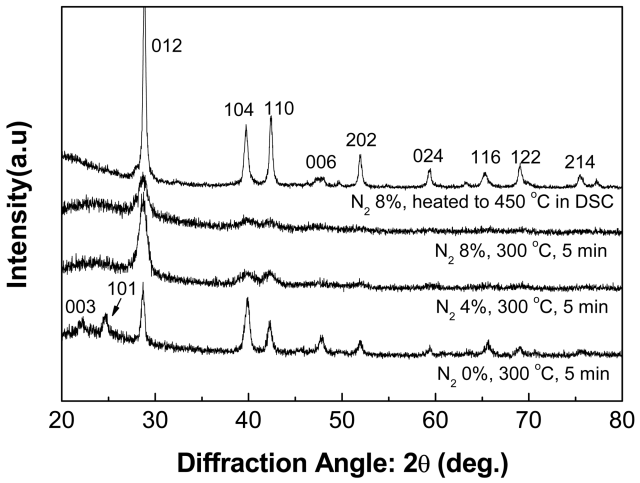

Fig. 2. X-ray diffraction spectra of the films sputtered with varying N_2 flow ratios and annealed at the conditions specified. Nearly all the peaks may be indexed according to a hexagonal crystal structure.

On closer inspection, the 2θ positions of the major peaks are essentially the same among films fabricated with different N_2 flow ratios, yielding a c/a ratio of around 2.672 (a: 4.265A, c: 11.398A and c/a ratio of the ideal rocksalt structure is 2.45). This suggests that nitrogen incorporation into the film may take place without giving rise to homogenous straining of the crystal lattice. Accordingly, significant line-broadening of the nitrogen-incorporated films annealed at 300 °C may be attributed to either fine crystal grains or non-uniform internal strain due to nitrogen incorporation. Among the films annealed at 300 °C, gradually decreasing peak

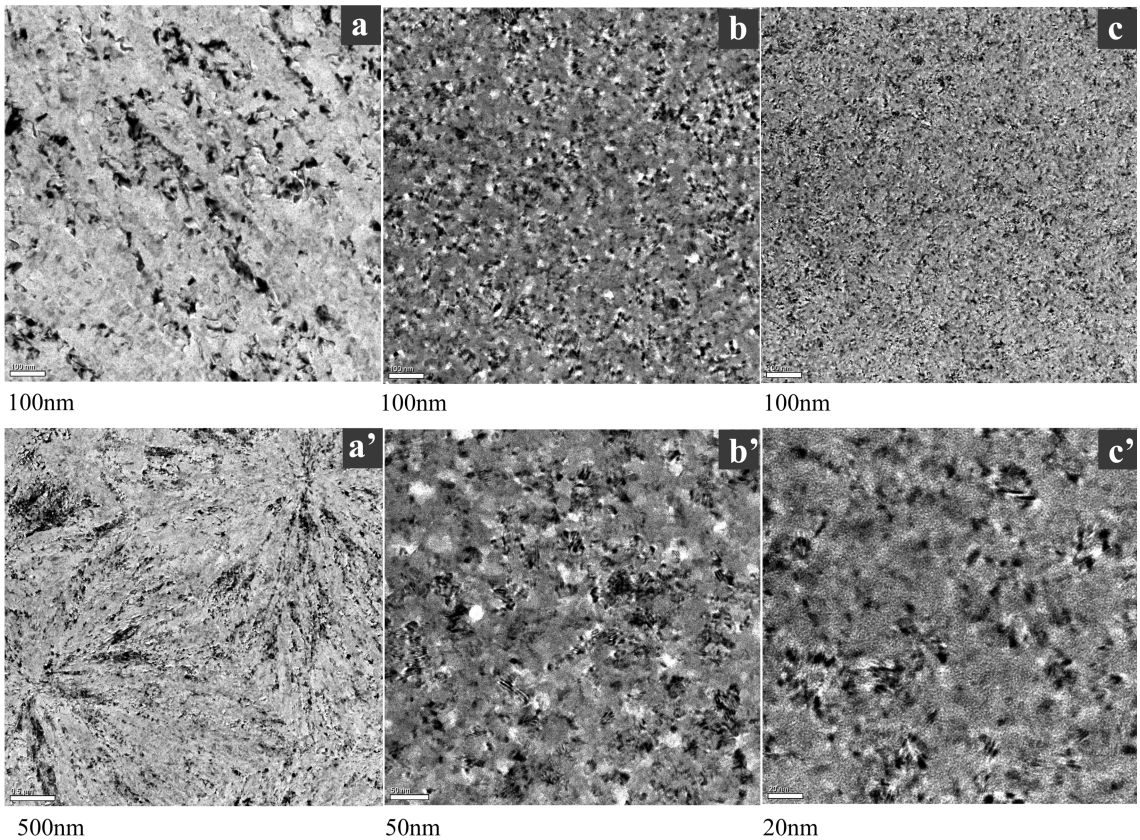

Fig. 3. TEM micrographs taken from the annealed thin film samples at 300 °C for 5 min made up of $ZnS.SiO_2$ (10 nm)/Ge-doped SbTe fabricated with varying N_2 flow ratios (20 nm)/$ZnS.SiO_2$(10nm) on a TEM grid: (a,a') 0% N_2; (b,b') 4% N_2; and (c,c') 8% N_2. Notice the increasingly fine microstructures and the presence of featureless amorphous-like contrast with increasing N_2 flow ratio.

intensities can be seen with increasing N_2 flow ratio, in conjunction with the equivalent trend observed for the first exothermic peaks in the DSC profiles. Both trends are presumed to signify progressively incomplete crystallization with increasing an N_2 flow ratio during the annealing process. In light of the fact that the DSC sample heated up to 450 °C produces peaks at the same 2θ positions as other films, but with smaller peak widths, it follows that the second exothermic peaks in Fig. 2 may be due to completion of crystallization accompanying the removal of the aforementioned causes leading to the x-ray line-broadening.

Figure 3 shows the TEM micrographs taken from the annealed thin film samples (at 300 °C for 5 min) made up of ZnS.SiO_2 (10 nm)/Ge-doped SbTe fabricated with varying N_2 flow ratios (20 nm)/ZnS.SiO_2(10 nm) on a TEM grid: (a, a') 0% N_2; (b, b') 4% N_2; and (c, c') 8% N_2. Consistent with x-ray line broadening, microstructures were found to become increasingly fine with increasing N_2 flow ratio. A lower magnification image (Fig. 3(a')) of the microstructures shown in Fig. 3(a) depicts a fully crystalline aggregate of a few micron-sized colonies, each displaying traces of interface-controlled growth in radial directions. In contrast, the microstructures shown in Fig. 3(b) and 3(c) appear to show a mixture of grainy features on a featureless background, which is suggestive of an untransformed amorphous phase. The presence of an amorphous phase is somewhat apparent from the high magnification image shown in Fig. 3(c'), an observation that agrees well with the weak x-ray peak intensities for the corresponding case (8% N_2, annealed at 300 °C for 5 min) in Fig. 2. From these observations, it follows that annealing at 300 °C for 5 min in fact results in incomplete crystallization of a film sputtered with a high N_2 flow ratio.

Accordingly, we may reach the following conclusion regarding the nature of the second exothermic peak that is shown to grow progressively to dominance with increasing N_2 flow ratio. Considering that the peak temperature of the second exothermic peak is sufficiently high (~0.8 T_m) and that crystallizations of the studied materials proceed predominantly by the motion of interface boundaries of sparse nuclei, the reaction in question may consist of growth and coarsening of crystalline grains by remobilization of the interface and/or grain boundaries that have been arrested for some reason.

3.3. Electronic Properties

Electrical resistivities of the as-deposited and the annealed films are plotted in Fig. 4(a) as a function of N_2 flow ratio. The resistivities of both films are found to increase initially with increasing nitrogen content while maintaining their ratios at around 10^5. Beyond 4% N_2, however, the rate of change in resistivity of the annealed films is found to slow down noticeably with a tendency for saturation. It is interesting to notice that the resistivities of the annealed films remain low in this regime, despite the presumed two-phase mixture state, which strongly suggests the possibility of percolating electrical conduction. On the nature of the resistivity changes of the annealed films, Fig. 4(b) clearly demonstrates that at an N_2 flow ratio of less than around 2%, the resistivity increase is entirely due to a decrease in Hall mobility, presumably resulting from enhanced grain boundary scattering in fine microstructures. As for a pronouncedly decreasing tendency in the rate of change of electrical resistivity beyond 4% N_2, a trade-off is observed between the opposing trends of changes in Hall mobility and carrier concentration. These opposing trends are typically expected when the boundaries do not comprise primary scattering centers. The decreasing carrier concentration with increasing N_2 flow ratio in this regime may be caused either by the increase in mobility gap (not shown here) due to the formation of covalent bonds by added nitrogen atoms or by the filling of some sort of acceptor-like traps with electrons of added nitrogen atoms, which would impede the generation of hole carriers.

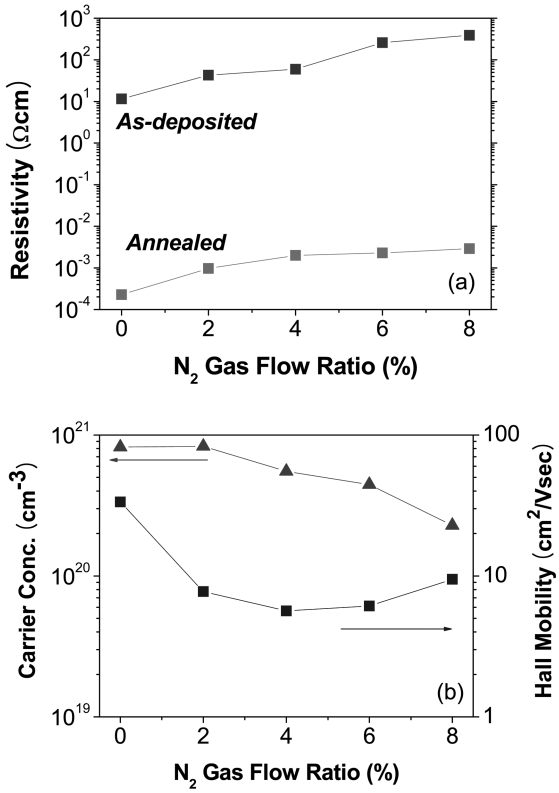

Fig. 4. (a) Electrical resistivities of as-deposited and annealed (at 300 °C for 5 min) films fabricated with varying N_2 flow ratios, (b) Carrier concentration and Hall mobility of annealed films fabricated with varying N_2 flow ratios. In conjunction with the resistivity change of annealed films, notice the gradual changeover from a rapid decrease in Hall mobility to a noticeable decrease in carrier concentration with increasing N_2 flow ratio.

3.4. Crystallization speed

The crystallization speeds of Ge-doped SbTe thin films fabricated with various N_2 flow ratios were compared with that of a $Ge_2Sb_2Te_5$ film of the same thickness. Using amorphous marks of varying size prepared by pulsed laser heating of varying power (P_w), reflectance was measured with time for each film during amorphous to crystalline phase changes with pulsed laser heating at some optimal powers (P_e) having ratios ranging from 0.6 to 0.8 relative to a respective critical power for melting (P_m). From the resulting plot, the required time for complete crystallization was determined at the intersection where a tangential line drawn at the time of maximum slope crosses a fiducial line representing the reflectance level of the fully crystalline background.

The results are shown in Fig. 5, which depicts the dependence of crystallization speed on P_w/P_m, that is, on the size of an amorphous mark. Among the group of Ge-doped SbTe materials of varying nitrogen content and $Ge_2Sb_2Te_5$, the differences appear categorical, representing characteristics of the two different modes of crystallization, *i.e.,* a growth-dominant mode and a nucleation-dominant mode[8]. Regarding the former group, it is emphasized that time for crystallization becomes dramatically reduced with P_w/P_m diminishing toward 1, to the extent that it becomes comparable to, or even less than, that of $Ge_2Sb_2Te_5$, depending on the nitrogen content. Films of higher nitrogen content display exceedingly longer time for complete crystallization in the regime of a larger P_w/P_m, which is consistent with the increasing trend in crystallization temperature with increasing N_2 flow ratio, as shown in Fig. 1. Yet, the observed difference almost vanishes in the regime of P_w/P_m approaching 1. Due to these remarkable scaling characteristics, Ge-doped SbTe materials with nitrogen addition could be applicable to a high-speed memory device having a progressively smaller programmable region.

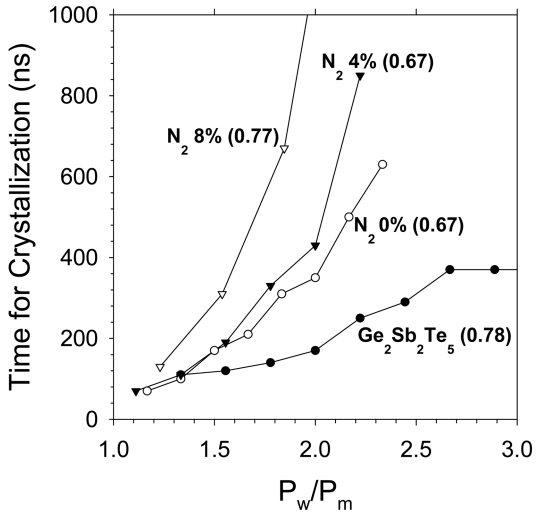

Fig. 5. Variation of crystallization time with respect to P_w (writing laser power)/P_m (critical power for melting) for various films specified; numbers in parentheses represent P_e (crystallizing laser power)/P_m. Notice the steep decrease in the crystallization time of Ge-doped SbTe films with diminishing P_w/P_m, which may probably lead to a crystallization speed comparable to or less than that of $Ge_2Sb_2Te_5$ in a high density memory with a tiny programmable region.

Some of the aforementioned property changes of the Ge-doped SbTe films with varying nitrogen content were found to be similar to those previously reported for the $Ge_2Sb_2Te_5$ films: increased resistivity[9], increased crystallization temperature[10], and progressively fine grains with increasing N_2 flow ratio[10]. In the crystalline states of both materials, the added nitrogen atoms are accommodated in inter-granular sites, such as interfaces and grain boundaries, or they are accommodated intra-granularly within grains. Besides, the crystal structures of both materials are akin to each other[7]. Accordingly, the structural mechanisms underlying the property changes are expected to be similar. Nevertheless, the difference of the crystallization mode seems to make nitrogen accommodation somewhat different between the two materials.

Added in a small amount to the Ge-doped SbTe material, nitrogen atoms are considered to enrich the moving interface boundaries of the crystal regions with an amorphous matrix and, subsequently, the grain boundaries in the course of transformation to a crystalline state. Since crystallization of the studied materials tends to proceed in the growth-dominant mode, nitrogen enrichment of the boundaries is most likely to impede the motion of boundaries that would require structural and compositional reconfiguration, and thereby leading to fine microstructures. This seems evident in light of a significant reduction in Hall mobility with little change in carrier concentration for a N_2 flow ratio of less than 4% N_2. This also appears consistent with the findings such as undisturbed melting temperatures and increased crystallization temperatures as made above from Fig. 1. In contrast, with a $Ge_2Sb_2Te_5$ phase-change material, the nitrogen enrichment of grain boundaries was presumed to occur via the formation of nitride phases, such as Ge-N, Sb-N, and Te-N when the nitrogen content exceeds a specific level[11]. As shown in the x-ray diffraction spectra of Fig. 2, however, no evidence of nitride phases was obtained in the present study.

With increasing nitrogen addition, significant intra-granular accommodation of nitrogen atoms seems to occur, as can be deduced from the decrease in carrier concentration beyond 4% N_2. As to the structural mechanism responsible for the property changes in this case, some insight can be gained from a proper understanding of the case with the rocksalt-like crystal structure of the $Ge_2Sb_2Te_5$ material. Concerning this, recall that the hexagonal crystal structure of the materials in the present study may be regarded as a rocksalt-like structure somewhat elongated along one 3-fold axis. Besides, these two structures are also chemically similar in the sense discussed below. A detailed structural model was

recently proposed by Kolobov *et al.* for the amorphization from and crystallization into the metastable rocksalt-like structure of $Ge_2Sb_2Te_5$ material[12]. Some building blocks of the model that are relevant to our discussion may be summarized as follows: 1) The rocksalt-like structure contains vacancies in the octahedral sites as intrinsic parts. 2) Charge redistribution around vacancies leads to local lattice distortions to produce longer Ge-Te and Sb-Te bonds that tend to be broken during melting. 3) During crystallization, a Ge atom neighboring a vacant site undergoes an 'umbrella flip' to move from a tetrahedral to an octahedral site.

As opposed to occupation of the tetrahedral sites, which is supposed in previous studies[9,10], we tend to believe that added nitrogen atoms would occupy octahedral vacant sites with some local displacements to form covalent bonds with surrounding atoms. This situation is energetically much more favorable, since no homogeneous straining of the lattice is involved. As a result, shifts in the positions of x-ray diffraction peaks would not be observed, except for some line-broadening (In fact, lattice distortion accompanying nitrogen addition was shown to be very small, *i.e.,* ~0.1% per 10 at% nitrogen addition, as shown in Fig. 4 of ref. [10]). Since melting of the material involves only atomic reconfiguration breaking the Ge-Te and Sb-Te longer bonds, the supposed occupation of nitrogen atoms in the octahedral vacant sites may cause little change in melting temperature. In addition, the crystallization temperature would increase, since the 'umbrella flip' might then interfere with the presence of a nitrogen atom in the vacant site. With modifications in the aforementioned building blocks to account for slight structural and compositional differences, property changes due to intra-granular accommodation of nitrogen atoms may be similarly explained in the case of Ge-doped SbTe materials.

4. SUMMARY

We have proposed Ge-doped SbTe with nitrogen addition as a representative phase-change material to overcome major technical challenges toward the development of a high-density phase-change memory. As compared with a nitrogen–free material, the nitrogen-added Ge-doped SbTe thin film materials were found to have promising material properties, such as increased electrical resistivity, increased crystallization temperature, with little change in melting temperature, and a crystallization time that is so scalable as to become reduced drastically as the size of a programmable region diminishes. From the dependence of the observed property changes on the N_2 flow ratio, we have suggested that accommodation of nitrogen may occur in two different ways: intergranularly and intra-granularly. In addition, the relative importance of one way of nitrogen accommodation over the other may vary with the amount of nitrogen addition and, apparently, between materials of two contrasting crystallization modes, *i.e.,* growth-dominant Ge-doped SbTe and nucleation-dominant $Ge_2Sb_2Te_5$. Careful structural and chemical characterization involving EXAFS and EELS measurements may clarify the mechanisms. Despite our observation of promising properties, the full potential of the studied materials can only be seen by way of memory device tests, which are being carried out presently.

ACKNOWLEDGEMENT

This work was supported by the National Research Program for 0.1 Terabit Non-volatile Memory Devices, sponsored by the Korean Ministry of Commerce, Industry, and Energy.

REFERENCES

1. M. Gill and T. Lowrey, J. Park, *Dig. Tech. papers of International Solid-State Circuits Conference*, p.202, TD 12.4 (2002).
2. F. Pellizzer, A. Pirovano, F. Ottogalli, M. Magistretti, M. Scaravaggi, P. Zuliani, M. Tosi, A. Benvenuti, P. Besana, S. Cadeo, T. Marangon, R. Morandi, R. Piva, A. Spandre, R. Zonca, A. Modelli, E. Varesi, T. Lowrey, A. Lacaita, G. Casagrande, P. Cappelletti, and R. Bez., *Proc. Symp. on VLSI Tech*. p.18 (2004).
3. S. J. Ahn, Y. J. Song, C. W. Jeong, J. M. Shin, Y. Fai, Y. N. Hwang, S. H. Lee, K. C. Ryoo, S. Y. Lee, J. H. Park, H. Horii, Y. H. Ha, J. H. Yi, B. J. Kuh, G. H. Koh, G. T. Jeong, H. S. Jeong, Kinam Kim, and B. I. Ryu, *Tech. Dig. of International Electron Device Meetings* p.907 (2004).
4. A. Pirovano, A. L. Lacaita, A. Benvenuti, F. Pellizzer, S. Hudgens, and R. Bez, *Tech. Dig. of International Electron Device Meetings* p.699 (2003).
5. M. H. R. Lankhorst, W. S. M. M. Ketelaars, and R. A. M. Wolters, *Nat. Mater.* **4**, 347 (2005).
6. T. D. Massalski, *Binary Alloy Phase Diagrams*, *2nd ed.,* ASM International, **3**, 3310 (1990).
7. H. Tashiro, M. Harigaya, K. Ito, M. Shinkai, K. Tani, N. Yiwata, A. Watada, N. Toyoshima, K. Makita, A. Kitano, and K. Kato, *Proc. of EPCOS.* (2003).
8. G. F. Zhou, H. J. Borg, J. C. N. Rijpers, M. H. R. Lankhorst, and J. J. L. Horikx, *SPIE,* **4090**, 108 (2000).
9. S. Privitera, E. Rimini, and R. Zonca, *Appl. Phys. Lett.* **85**, 3044 (2004).
10. T. H. Jeong, M. R. Kim, H. Seo, J. W. Park, and C. Yeon, *Jpn. J. Apply. Phys.* **39**, 2775 (2000).
11. R. Kojima, S. Okabayashi, T. Kashihara, K. Horai, T. Matsunaga, E. Ohno, N. Yamada, and T. Ohta, *Jpn. J. Appl. Phys*. **37**, 2098 (1998).
12. A. V. Kolobov, P. Fons, A. I. Fenkel., A. L. Ankudinov, J. Tominaga, and T. Uruga, *Nat. Mater.* **3**, 703 (2004).